# We are IntechOpen, the world's leading publisher of Open Access books Built by scientists, for scientists

6,900
Open access books available

185,000
International authors and editors

200M
Downloads

Our authors are among the

154
Countries delivered to

TOP 1%
most cited scientists

12.2%
Contributors from top 500 universities


WEB OF SCIENCE™

Selection of our books indexed in the Book Citation Index in Web of Science™ Core Collection (BKCI)

## Interested in publishing with us?
## Contact book.department@intechopen.com

Numbers displayed above are based on latest data collected.
For more information visit www.intechopen.com

Chapter 2

# Multiscale Meteorological Systems Resulted in Meteorological Tsunamis

Kenji Tanaka and Daiki Ito

Additional information is available at the end of the chapter

http://dx.doi.org/10.5772/63762

**Abstract**

Meteorological tsunami is a kind of the ocean long wave with the tsunami frequency band from several minutes to 2 h driven by atmospheric forcing at the sea interface. The multiplying of resonance and amplification effects enhanced the wave higher than 1 m with the destructive damage. The direct forcing of meteorological tsunami is the meso-β-scale disturbance, such as mesoscale convection system or internal gravity wave in the troposphere. The events on the destructive meteorological tsunamis were reported mainly on the mid-latitude regions such as Europe and US East Coast. Whatever the kind of the disturbance was, the intrusion of the dry air played important roles in unstable structure of the middle troposphere to travel the disturbance with a long disturbance. The backward trajectory of the air particle on the tsunami-enhancing region showed that the lifting of anomalous warm moist air mass from the lower latitude was significant to form the atmospheric structure over the targeted seas. Such characteristics in the large-scale atmosphere provide the possibility of the mid-term prediction on meteorological tsunamis, linking with the state-of-art observation technologies in satellite remote sensing, radar observation, in situ measurement network and so on.

**Keywords:** meteorological tsunami, inverse pressure effect, resonance, meso-β-scale disturbances, convective systems, atmospheric internal gravity wave, continental scale circulation

## 1. Introduction

Meteorological tsunami (or meteotsunami) is a kind of ocean long wave with the tsunami frequency bands from several minutes to 2 h driven by atmospheric forcing such as the disturbance of sea level pressure, wind, and others [1, 2]. The sea level rises (or depresses) inside

INTECH
open science | open minds

© 2016 The Author(s). Licensee InTech. This chapter is distributed under the terms of the Creative Commons Attribution License (http://creativecommons.org/licenses/by/3.0), which permits unrestricted use, distribution, and reproduction in any medium, provided the original work is properly cited. CC BY

of the negative (positive) pressure anomalies. The sea level also rises accordingly with the horizontal convergence of the wind stress, for example, around the front or the coastal area. Such basic mechanism to set the wave up is similar as the storm surge. But the period of the storm surge is as long as tidal motion (approximately half or 1 day), while that of meteorological tsunami is generally much shorter than tidal motion. The intensity of the sea level deformation by severe storm is typically as large as several 10 cm or higher than 1 m including wind stress. But the intensity itself of the forcing to meteorological tsunami is much smaller than that related to storm surge: an order of several centimetres in typical cases. The multiple mechanism of the resonance at the sea interface enlarges the amplitude of the ocean long waves, and the wave will possibly become higher than 3 m with flooding and destruction of the dikes. The primitive mechanisms on meteorological tsunami are founded by geophysicists in the earlier and middle twentieth century [2–4]. In recent decades, however, the integration of the scientific findings throughout severe case studies and the advances in field observation, numerical modelling and data assimilation have revealed the significance of the multiscale mechanisms on atmospheric and oceanographic processes.

In the present chapter, we briefly introduce resonant mechanisms as propagating meteorological tsunamis. Next, we show the area where destructive meteorological tsunamis have been reported. After that, we present the various kinds of the weather conditions resulting in meteorological tsunamis. **Figure 1** indicates the typical scale of meteorological phenomena and oceanographic motion. The temporal scale of meteorological tsunami typically matches the meso-β-scale motion in the atmosphere such as squall line, internal gravity wave, gravitational flow and so on. However, the genesis of those motion is influenced by both smaller- and larger-scale motions. The organization of turbulent plume will generate the cumulus convection, and cluster of the convective cells will form the meso-β-scale system.

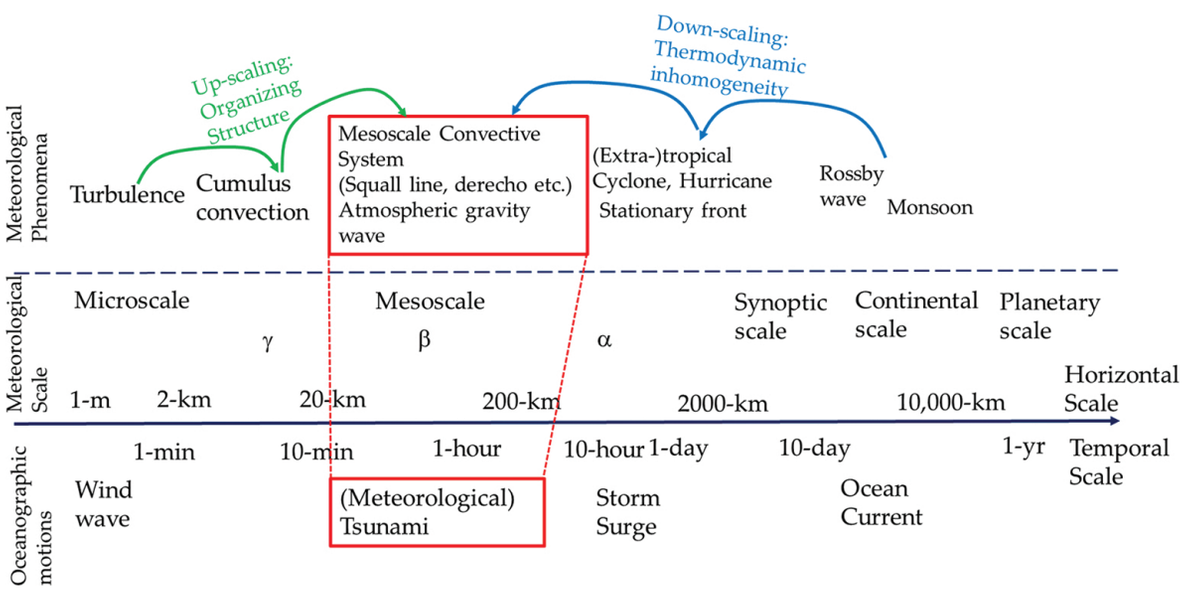


**Figure 1.** Scale of the various meteorological phenomena, and oceanographic motions.

The larger-scale motion provides the atmospheric instability structure by mixing dry air and moist air mass, that is, thermodynamic inhomogeneity. Hence, we first present the mesoscale phenomena resulting in meteorological tsunami, and then we discuss the meteorological phenomena including the large-scale motion (synoptic or continental scale). After that, we discuss and conclude the predictability of the meteorological tsunami with the current technologies on field observation, numerical modelling and data assimilation.

## 2. Resonant and amplifying mechanisms of the meteorological tsunami

### 2.1. Proudman resonance

One of the most important resonances was derived by Proudman (1929) [4], which is a coupling of the ocean long wave and the atmospheric disturbance. Let $U$ the propagation speed of the pressure disturbance, and $c = (gH)^{1/2}$, the phase velocity of the ocean long wave dependent on the ocean depth $H$ and the acceleration of the gravity, $g$. The Froude number Fr is defined as the ratio between the atmospheric motion and the ocean wave propagation, $\mathrm{Fr} = U/c$. Assuming that the friction, Coriolis, eddy viscosity and advection terms can be negligible (i.e. one-dimensional (1D) linear wave), the normalized sea level change becomes

$$\frac{\eta}{\eta_s} = \frac{1}{1 - Fr^2} \tag{1}$$

in equilibrium, where $\eta_S = -\Delta P/\rho g$ the sea level change under static balance with the intensity of the pressure anomaly $\Delta P$ and the density of water $\rho$. Equation (1) implies that sea surface can be deformed unlimitedly as the pressure disturbance moves the ocean with the same speed of the phase velocity of the long wave (i.e. holding Fr ~1).

When Fr ~1, the work due to the atmospheric pressure gradient force supplies wave energy at the same phase continuously, and the magnitude of the sea level deformation will be proportional to the travelling distance of the pressure disturbance on the sea interface. If $U > c$, that is, Fr > 1, that is, supercritical propagation over very shallow water, a wake forms similar to that passing the vessel with high speed. On the other hand, the subcritical propagation such that $U < c$, the ocean long wave will propagate ahead of the atmospheric disturbance, with the wave length becoming longer and longer instead of enlarging the amplitude.

The effect of the Proudman resonance typically ranged from two to five times of the stationary state. When the atmospheric disturbance travels longer than 1000 km keeping Fr =1 ± 0.10, the resonant effect can be higher than 10 times of the stationary state. Hibiya and Kajiura (1982) [5] derived the formula under the condition of Fr ~1 as,

$$\frac{\eta}{\eta_s} = \frac{1}{2}\frac{X_f}{W} \tag{2}$$

where $X_f$ represents the fetch of the pressure disturbance, and $W$ is the width of the pressure disturbance. For example, $X_f$ = 500 km, $W$ = 50 km yields the amplification ratio $\eta/\eta_s$ = 5.0.

### 2.2. Shoaling and refraction

Similar to seismic tsunami, meteorological tsunami is also amplified by shoaling and refraction. Linear theory can be used as the first approximation to calculate the wave height as the wave moves across an ocean and undergoes wave shoaling and refraction. The formula can be written as (e.g. Synolakis, 1991 [6])

$$\frac{\eta_p}{\eta_o} = \left(\frac{D_o}{D_p}\right)^{\frac{1}{4}}\left(\frac{B_o}{B_p}\right)^{\frac{1}{2}} \tag{3}$$

where $\eta_o$ = wave height (crest to trough) at the original point, $\eta_p$ = wave height (crest to trough) at any point, $D_o$ = water depth at source point, $D_p$ = water depth at any shoreward point, $B_o$ distance between wave orthogonals at a source point of water and $B_P$ = distance between wave orthogonals at any shoreward point of water. The ratio between $B_o$ and $B_p$ indicates the refraction, and the ratio between water depth indicates the shoaling, a part of Green's law.

### 2.3. Resonance of the edge wave

The resonance due to continental shelf is also significant in amplifying the meteorological tsunamis. For example, Greenspan (1956) [7] derived the surface elevation across the continental shelf from the linearized shallow water equation. Let the beach slope $\alpha$ = tan $\beta$, and $U$ = velocity of pressure disturbance along the edge, the frequency of $n$-th edge mode can be described as

$$\mathrm{k_n} = (2n+1)g\alpha / U^2 \tag{4}$$

Giving the pressure distribution as a Gaussian function moving along the shelf edge, the amplitude of the $n$-th edge wave depends (with the wave number of $k_n$) on the intensity of the pressure disturbance $P_0$, the moving speed of the system, horizontal scale of the disturbance $a$ and the distance from the coast line $y$ as

$$\mathrm{A_n}(k_n) = -\frac{2}{U}\left(-\frac{2\sqrt{\pi}UP_0a}{\rho}\right)k_n^2\exp\left(-\frac{a^2k_n^2}{4}\right)\int_0^\infty L_n(2k_ny)\exp\left\{-k_ny-\frac{(y-y_o)^2}{a^2}\right\}dy \tag{5}$$

where

$$L_n(s) = \exp(s)\left(\frac{d^n}{ds^n}\right)\left(s^n \exp(-s)\right) \tag{6}$$

For fundamental edge mode ($n$ = 0), the maximum wave height becomes maximum with the half-pressure radius of 80–90 km. This implies that the meso-β- or γ-scale disturbance, the typical wavelength of the meteorological tsunami, is able to amplify the wave by edge mode rather than meso-α-scale disturbance such as hurricane.

### 2.4. Harbour resonance

The resonance in the harbour or the inlet is the conclusive effect of how much sea level oscillates inside them. Assuming that the bay shapes rectangular open channel with uniform sea depth ($H$), and the incident direction of the ocean wave is parallel to that of the axis of the bay. The period ($T$) for eigen oscillation of the bay is

$$T = \varepsilon \frac{4L}{n\sqrt{gH}} \tag{7}$$

with $L$ = axis length of the bay. The coefficient $\varepsilon$ represents the correction coefficient for the bay mouth effect due to the generation of scattering waves near the bay of the mouth [8] as

$$\varepsilon = \left[1 + \frac{2B}{\pi L}\left(0.923 + \ln\frac{4L}{\pi B}\right)\right]^{\frac{1}{2}} \tag{8}$$

where $B$ = the width of the bay mouth. For more details, refer to Ravinobich (2009) [9] for the various shapes of the inlets.

## 3. Meteorological tsunami in the world ocean

The area where large meteorological tsunamis with the destructive damages were reported is marked in **Figure 2**. The colour palette in **Figure 2** indicates the phase speed of the ocean long wave $c = (gH)^{1/2}$, instead of the sea depth. Much of the events occurred in the mid-latitude, where the energy transport towards polar region is the most active throughout the meridional circulation. The wind speed of the mid-troposphere typically ranges 20–40 m/s along with the westerly jets, which is dominant to propagate the meso-β- or γ-scale atmospheric disturbance at sea level.

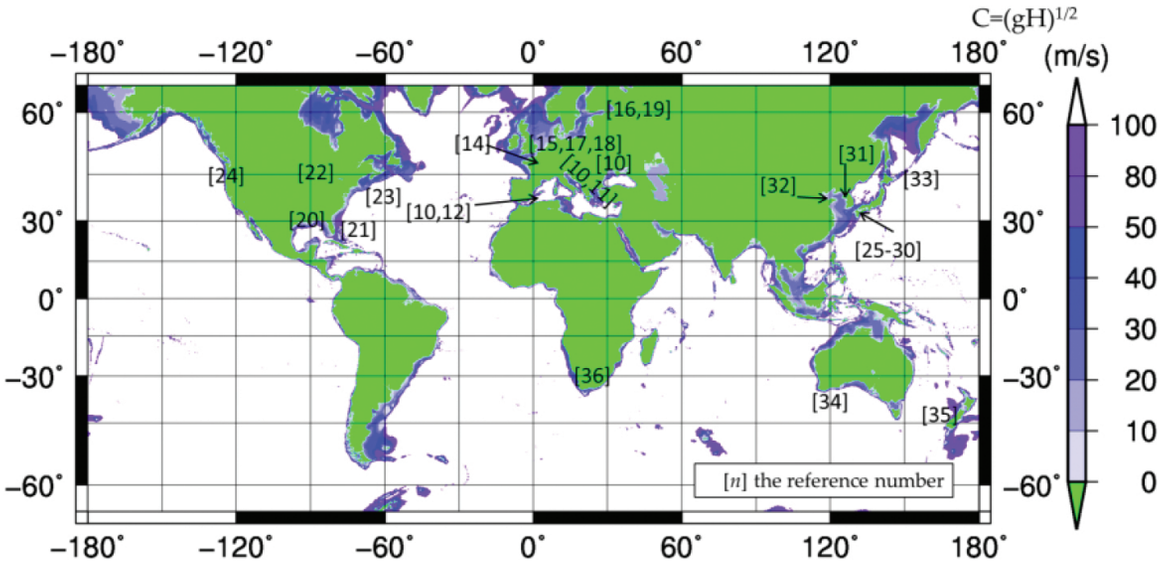


**Figure 2.** Map of the destructive meteorological tsunami events in the world. Colour shows the propagation speed of the ocean long wave $c = (gH)^{1/2}$ using the bathymetry of ETOPO5. Numbers indicate the location of event of the related references cited in this section.

Vera Luka, Croatia, June 1978
Vilibić et al. (2009)[11]

Ciutadella Harbour, Menorca Is.
Spain, June 2008 Vilibić et al. (2008)[12]

**Figure 3.** Example of scenes on destructive meteorological tsunami [11, 12].

The Mediterranean Sea including Adriatic Sea is one of the hotspots of the meteorological tsunamis. One of the recent major events occurred on 23–27 June 2014 due to the internal gravity wave (IGW) of the mid- and low troposphere [10]. In that event, the wave height became as high as 2–3 m in the wide area of the sea. The atmospheric IGW propagated not only over the Mediterranean Sea but extended to the Black Sea. The east coast of the Adriatic Sea, Croatia (*šćiga* in local name) has many small islands and complicated shoreline shape with small bays (smaller than 10 km in axis length) and has suffered from severe events. The most severe event in June 1978 brought the maximum wave height as high as 6 m [11]. At least five destructive events with the inundation damage occurred other than 2014 event: in June 1978 at Vera Luka

http://dx.doi.org/10.5772/63762

with 3-m wave height, in October 1984 at Ist Island with 4-m wave, in June 2003 over the middle Adriatic coast with approximately 3.5-m wave, in August 2007 at Ist Island with 4-m wave and in 2008 at Mali Lošinj [11]. The Balearic Island (*rissaga* or *resaca* in local name) is the area where large amplified waves hit as frequent as the Adriatic Sea. The large wave as high as 2 m hit that area once per 5–6 years. And 3–4-m waves hit once per 20–30 years. June 2006 event was the most severe one in recent decades: the wave as high as 4–5 m hit the the Ciudadella Harbour of the Menorca Island located in the east of the Balearic Islands [12]. An example of meteotsunami damages in those two areas is shown in **Figure 3**. Hundreds of fishing boats were destroyed by strong current, and hundreds of motorcars and number of residences were damaged by flood. Other coast at Sicily in Italy (*marrubio* in local name) and at Marta (*milghubo* in local name) also recorded wave height higher than 1 m in hitting the meteorological tsunamis [13].

Much of the large meteorological tsunami events had been reported over the coastal area of the northwest Europe, but not so frequent as compared to the Mediterranean Sea region. Since the shallow seafloor extended in the northwest Europe, it is easier for the wave to enhance by the Proudman resonance. Haslett et al. (2009) [14] summarized 9 events of the possible meteorological tsunamis over past 120 years in the United Kingdom. The recorded wave height ranged 4–9 m, caused mainly by squally thunderstorms. According to their paper, the sudden sea level rise within 5–10 min was reported. That time was too long to period of swell with the period around 10 s or little bit longer. The amplification effect in shoaling at the continental shelves of the Atlantic Ocean seemed to play an important role in the enhancement of the meteorological tsunamis. Much of the meteorological tsunami events were recorded in the South Wales and South England, where the channel opens to the west (Atlantic Ocean). The squall lines along with cold front in developed extratropical low sometimes bring the meteorological tsunamis in the southern North Sea [15] (*zeebeer* in Netherland, *seebär* in Germany) and Baltic Sea (*seebär* in Germany, or *sjösprång* in Swedish) [16]. The major recent event was brought by the cold front passed over the Netherland and Belgium on January 3, 2012. According to the weather information service webs in Netherland, sudden depression of the tide level was recorded by 1.66 m per 20 min at van Rijkswaterstaat [17], while the sudden rise of the tide level was recorded by 1.05 m per 20 min in Ijmuiden [18]. In the coastal area of the Finland, the latest major event brought the wave higher than 1.0 m (10–15 min in period) on July 29, 2010. The meteorological tsunami up to 1.5 m in wave height was also reported in May 15, 1924, caused by thunderstorm [19].

The developed squall line system or the atmospheric gravity waves brought the meteorological tsunamis in the wide area of East Coast of the United States including the Florida Peninsula and Gulf of Mexico [20, 21]. On March 1995, the giant meteorological tsunami with a 3.3-m wave height hit along the east coast of the Gulf of Mexico, Florida, due to the atmospheric gravity waves propagated from the Texas-Louisiana thunderstorm [20]. The derecho developed at the inland area of the North US brought the meteorological tsunamis not only in the Atlantic Ocean but also in the Great Lakes [22]. The meteorological tsunami on the Great Lakes as large as 3 m in wave height recorded on by squall line passage in June 1954 even the lateral extent was not so wide (~250 km) as compared to the continental shelves in Atlantic Ocean [23].

The west coast of United States has complicated shoreline shapes, similar to the Adriatic Coasts. However, the wave amplitude for each event was not so large [24].

East Asia region is one of the major spots of meteorological tsunami. There are several characteristics that can enhance meteotsunami much easier than other coastal regions. The unstable layer in the middle troposphere can easily form because a couple of jets in the upper air get closed in the leeward of the Tibetan Plateau. The lifting of the wet moist air from lower latitude and the descending of the upper dry air from continental region makes the so-called wave-ducting layer often. A wide coastal continental shelf is extended from China to the Islands of Japan. The equivalent speed of the ocean long wave ranged 20–40 m/s except the Okinawa trough near the Kyushu Island, Japan. What is more, there are many small inlets having eigen periods ranging between several minutes and several hours. In March 1979, a giant meteorological tsunami (*abiki* in local name) hit on the Nagasaki Bay in Kyushu, Japan, by passing abrupt pressure jump of 5.9 hPa per 30 min. The tide gauge observed the maximum wave height of 2.78 m [25]. A large meteorological tsunami also caused by train of pressure wave with the amplitude of 0.5–2.0 hPa, with the wave length of 20–100 km [26, 27]. In the west Kyushu, most of meteorological tsunami are likely observed in the season between February and early April [28, 29]; however, the severe squall system such as Baiu front sometimes generates the strong downdraft to meteorological tsunamis [30]. On the west of the Korean Peninsula, maximum amplitude of 1.4–1.6 m recorded in March 2007 and May 2008 with the pressure jump of 2–5 hPa travelled over the Yellow Sea [31]. In the Bohai Sea of China, sea level oscillations with the amplitude higher than 1.0 m are often observed; however, the oscillation period was much longer (56–160 min) than that reported in other coasts (nearly 5–20 min). Such large amplified oscillation remained unclear as to what kind of the atmospheric sources induces such a long period wave [32]. The meteorological tsunami hit on the Kuril Island and the Kamchatka when the developing low approached the area from Hokkaido, Japan. In recent years, the wave height recorded was higher than 1.2 m in February 2010 [33].

Some destructive events have been introduced in recent papers, which occurred on the southern hemisphere. The west coast of Australia caused the meteorological tsunami resulting from squall line or frontal passage in the low pressure system. The wave height of 1.0 m was recorded in the frontal passage on June 12, 2012 [34]. Similar magnitude of meteorological tsunami was measured on the coast of New Zealand in April 2002 (*rissaga* in local name) [35]. A large flooding damage by meteorological tsunami 2.9-m wave height occurred on the west coast of South Africa on August 7, 1969. In that event, the flooding damage of housings and parked automobiles was brought within the area of 2 km along the shoreline and 100–200 m across the shoreline due to run-up of the wave [36].

It is possible that other coastal areas hit the meteorological tsunami if the multiple resonant conditions were satisfied. However, the recorded wave height were smaller than 1-m in those coastal areas. For example, Pattriaratki and Wijeratne (2015) [14] introduced smaller meteotsunamis in the tropical region such as Sri Lanka and India.

http://dx.doi.org/10.5772/63762

## 4. Mesoscale convective systems

The mesoscale convective system (MCS) is one of the most important phenomena to generate pressure jumps at sea level. The horizontal scale of the individual convective cell is an order of ~10 km, with the lifetime of several tens of minutes. The vertical wind speed sometimes becomes as high as 20 m/s under the strong unstable atmosphere with the convective available potential energy (CAPE) higher than 1000 J/kg. A high pressure anomaly, of the order of 1–2 hPa, generates at the surface level inside the convective cell due to the downdraft. To travel a long distance satisfying the Proudman resonance, it is significant to form a series of the convective system including multiple cells such as squall line.

Derecho is one of the systems with a long lifetime, which can move fast and long enough to have Proudman resonance on the ocean surface. The lifetime of the derecho is longer than 6 h travelling hundreds to thousands of kilometres as seen in **Figure 4** [20]. Some of the severe systems bring very strong gusts higher than 40 m/s (~90 miles/h) with the destructive damage of housings in the land area. A schematic of the derecho structure and sea level pressure fluctuation is shown in **Figure 5** [37]. The organized convective systems move towards the warm sector parallel to low-level thickness lines with the mean tropospheric flow. The system moves as high as 15–25 m/s (50–90 km/h), when the velocity of the mean tropospheric flow is very fast against the horizontal wind velocity of the low-level moist air into the convective system.

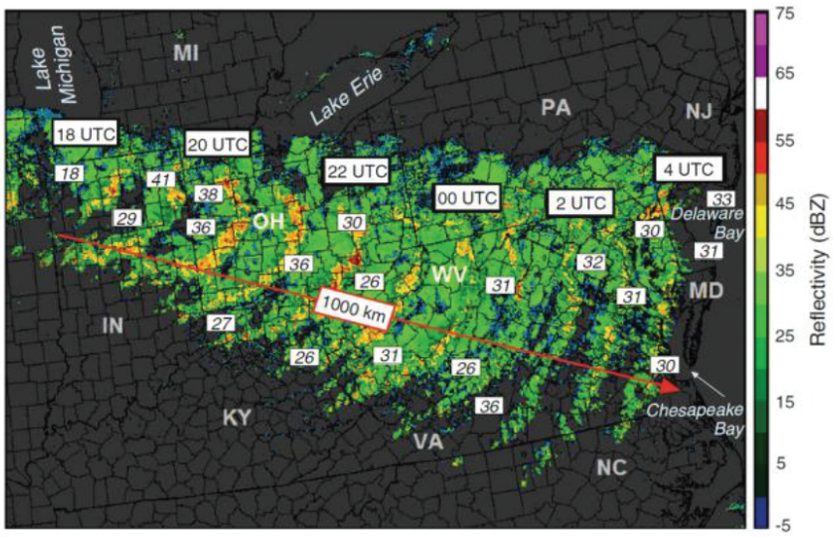


**Figure 4.** A mosaic composite of radar reflectivity (dBZ) image indicating the development and evolution of the derecho during June 29 and 30, 2012. Unitless numerical values indicate observed wind gusts (m/s). (Image by G. Carbin, NOAA/NWS Storm Prediction Center [22]).

In the US East Coast, the derecho had moved from land to ocean and the tsunami propagated towards offshore with Proudman resonance. **Figure 6** shows a sequence of the wave propagation simulated by the Pacific Tsunami Warning Centre, NOAA, as an example of June 13, 2013 [38]. The body wave, surrounded by a rectangle marked as 'a', generated along the coast

of Philadelphia (see the upper left panel in **Figure 6**) and moved eastward over the continental shelf. The wave was reflected along with the edge of the continental shelf and back to the coast. The body wave propagated across the edge after 17:00Z, crossing with the reflected wave. The body wave seemed to have disappeared at 20:00Z, which travelled longer than 300 km along the coastal shelf. The area of the maximum wave height higher than 10 cm corresponded with the area passing the body wave with resonance effect.

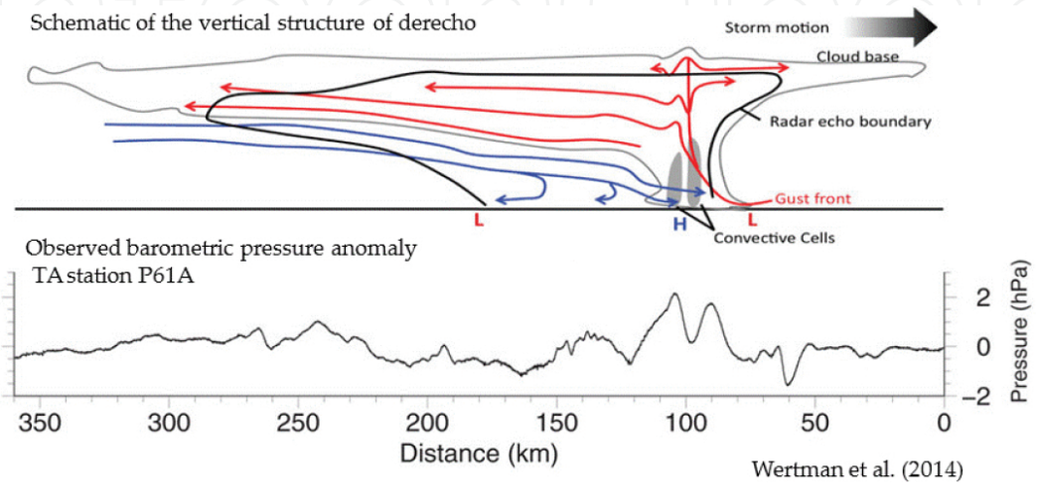


**Figure 5.** A schematic of the vertical structure of derecho (upper panel) and observed barometric pressure anomaly during the passage of derecho (lower panel) after case study on June 13, 2013 event, by Wertman et al. (2014) [37].

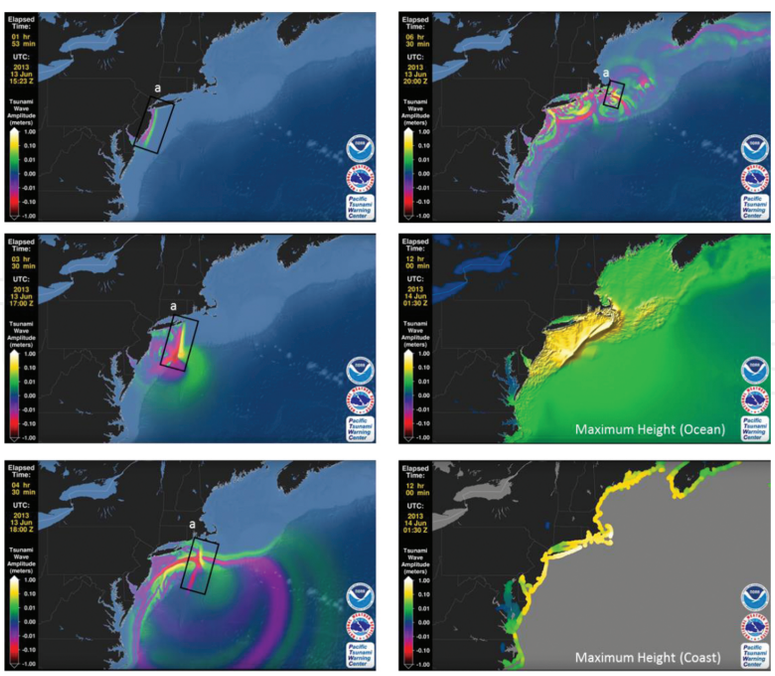


**Figure 6.** A sequence of the meteorological tsunami propagation computed by NOAA Pacific Tsunami Warning Centre. (Available from https://www.youtube.com/watch?v=ykABRe5Yt3c [38]).

http://dx.doi.org/10.5772/63762

## 5. Pressure jump of Nagasaki 1979 'Abiki' event

The system with the strong intrusion of the cold dry air can cause the abrupt pressure jumps with weak precipitation or without precipitation. **Figure 7** shows the satellite image and the observation records of meteorological tsunami by abrupt pressure jumps at Nagasaki Bay in west Kyushu, Japan [25]. The maximum wave height showed 278 cm at the third wave in tidal station of Nagasaki port. Some references cited the maximum wave of 4.8 m at this event [14], but that value was estimated value using Green's formula in Eq. (3). Abrupt pressure jump of 5.9 hPa per 30 min was recorded at Meshima about 140 km southwest from Nagasaki. The pressure jump decayed as the system moved to east and the intensity was 3.0 hPa per 20 min. Hibiya and Kajiura (1982) [5] proposed that the pressure jump was generated at the region near Shanghai, China, while Akamatsu (1982) [25] suggested that pressure jump was generated more towards the east side near Meshima. The satellite visible image showed that there was clear boundary between the stratiform cloud and the dry air in the middle of the East China Sea.

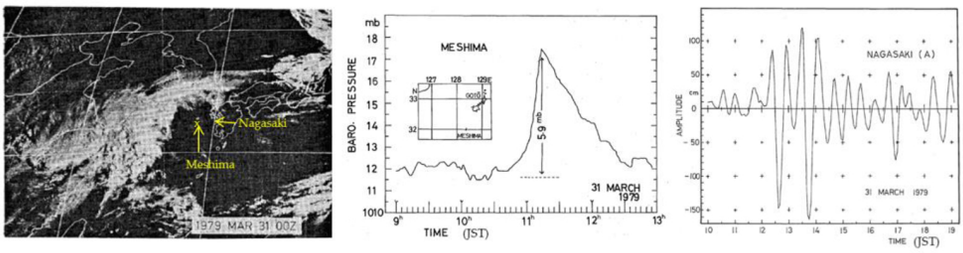


**Figure 7.** Meteorological tsunami of Nagasaki Bay caused by abrupt pressure jump on March 31, 1979. Satellite visible image by Geostationary Meteorological Satellite (left), barometric pressure recorded at Meshima (middle) and tidal amplitude observed at Nagasaki Bay (right) (Akamatsu 1982) [25].

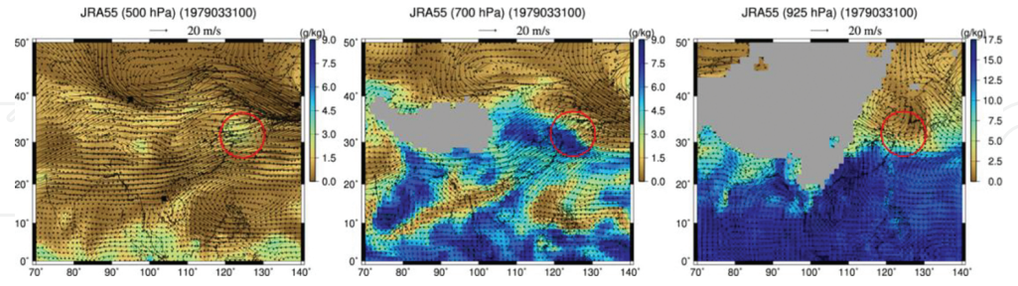


**Figure 8.** Distribution of the wet and dry air and horizontal wind in 500 hPa (left), 700 hPa (middle) and 925 hPa (right) isobar surface on 00Z, March 31, 1979. The reanalysis data of JRA-55 (Kobayashi et al. 2015) [39] was used.

The long-term reanalysis data from Japan Meteorological Agency (JRA-55) [39] in **Figure 8** indicated that the lower troposphere over the East China Sea was very dry (smaller than 3 g/kg in mixing ratio) and moist air came from south China region in 700 hPa isobar surfaces. The moist air lifted upward orographically in the mountain range of south China and vapour front formed in the mid-troposphere. Around the vapour front, the dry air cooled by re-

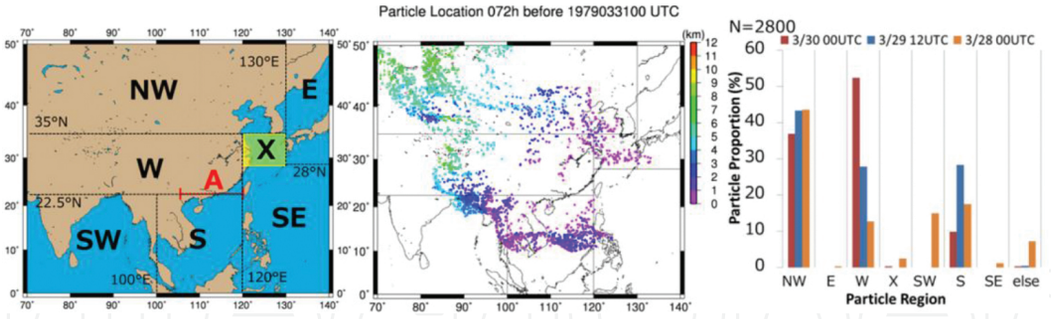


**Figure 9.** Air particle distribution into East China Sea. The left panel indicates the analysis area with initial particles located in region X. The middle panel shows the distribution of the individual particles 72 h before the meteorological tsunami over the East China Sea. The colour markers indicate the altitude of each air particles. The right panel indicates the particle proportion in each sector shown in the left panel [26].

evaporation of the cloud liquid water and settled down. The pressure jump was generated in the dry sector of the vapour front in the mid-troposphere. The back trajectory analysis of the air particle [39] depicted in **Figure 9** showed that the air particle in the East China Sea during the meteotsunami event came from mainly two or three regions. The warm moist air mainly came from South China Sea, Indochina Peninsula and Bengal Bay. Those air particles moved northeast along with the high-pressure system located in the Philippines, and lifted orographically over the inland area of the South China (region 'SW' and 'S'). Other particles came from upper dry air of northwest Eurasian continent or along with the subtropical jets via Tibetan Plateau (region 'NE' and 'E'). Further analysis in **Figure 10** showed that the anomalous mass of the moist air in the lower troposphere was transported from the tropical regions within 3 days before the meteotsunami event on March 31, 1979. The peak value of the moisture transport in the end of March (~200 kgm/s) was much greater than the peak value in the summer monsoon season (~150 kgm/s). The massive transport of the lower moist air into inland China can be seen especially in the late winter and early spring (February–April) for nearly every year. In the same period, the secondary oscillations larger than 1.0 m in amplitude were

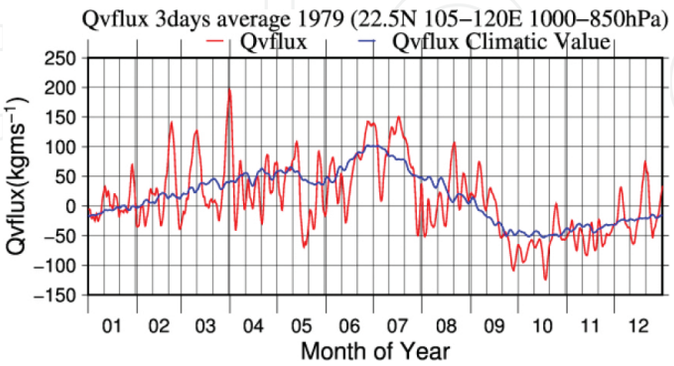


**Figure 10.** The northward component of water vapour flux across the line of South China coasts (22.5N, 105–120E) after the vertical integration between 850- and 1000-hPa isobar surface. Red line indicates the 3-day average from 6-h data in the year 1979. Blue line indicates the 10-day average of climatic value for 55 years (1958–2012) [26].

http://dx.doi.org/10.5772/63762

measured in the west Kyushu [27] nearly for every year. Hence, fluctuation of the vapour transport from tropical region to inland China can be key information to provide the first guess of the atmospheric disturbance causing meteorological tsunamis.

## 6. Atmospheric gravity waves in the troposphere

The atmospheric gravity waves are also one of the typical processes to generate pressure disturbance in the sea level, travelling with a long disturbances. There are two mechanisms supporting such characteristics of the atmospheric gravity wave: wave duct [40] and wave CISK [41]. The stable lower troposphere with an increasing wind in a vertical direction is overtopped with an unstable layer in the mid-troposphere as illustrated in **Figure 11** [10]. The Richardson number Ri

$$Ri = \frac{N^2}{\left(dU / dz\right)^2} \tag{9}$$

is generally used to see the atmospheric stability, where $N$ = the Brunt-Väisälä frequency and $U$ = horizontal velocity. Such vertical structure reflects the wave energy and traps the gravity waves towards the long distance [40, 42, 43]. The potential for downward or upward propagation of mid-tropospheric internal gravity waves may be assessed from the inequality of the linear gravity wave theory [43, 44].

$$N > \frac{2\pi U}{\lambda} \tag{10}$$

where $\lambda$ = the horizontal wavelength of internal gravity wave. The depth of the wave duct D is described as

$$D = \lambda_z \left(\frac{1}{4} + \frac{1}{2}n\right) \qquad (n = 0,1,2,....), \tag{11}$$

where $\lambda_z$ denotes the vertical wave length. Using the wind speed at critical level $U_c$, the $\lambda_z$ can be approximated as

$$\lambda_z \approx 2\pi \frac{U_c - U}{N} \tag{12}$$

The wave CISK denotes the coupling between the gravity wave and convection. The convergences associated with the gravity wave force the moist convection while convection heating provides the energy for the wave [26, 41, 45].

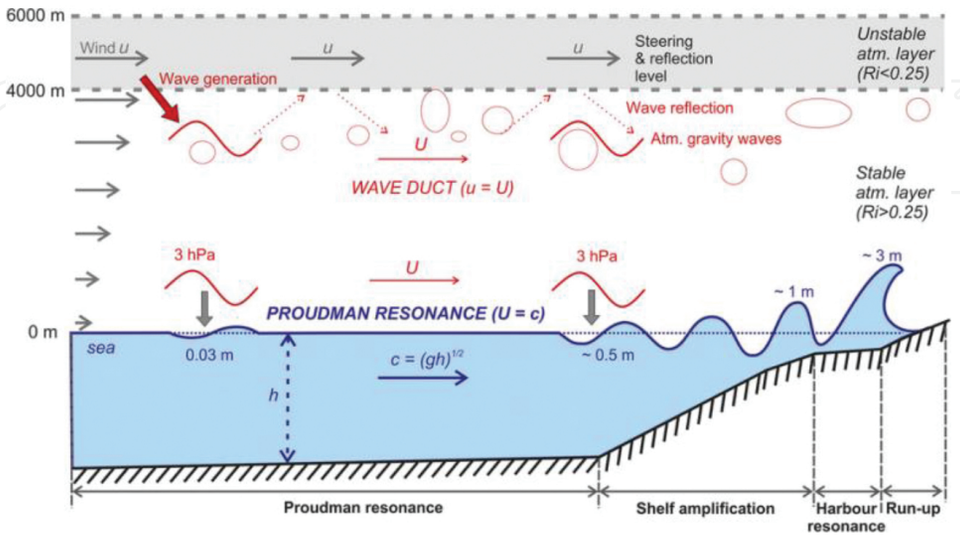


**Figure 11.** Schematic of the generation and the propagation of the atmospheric gravity wave in the presence of the wave-ducting layer, and the enhancement of the ocean long wave. A case study for widespread meteorological tsunami on Mediterranean and Black Sea, in June 2014 (Šepić et al., 2015) [10].

The large-scale motions with meso-$\alpha$ scale, synoptic scale or monsoon scale provide the structure of wave-ducting layer or wave CISK. In June 2014 event, the expansion of the wave-ducting layer generates and propagates the atmospheric gravity waves. The synoptic weather pattern and the sea level oscillation in that event are shown in **Figure 12** [10]. According to the Šepić et al. (2015) [10], the synoptic structure can be summarized as follows: first, inflows of warm and dry air from Africa in the low troposphere (~850 hPa); second, a strong south-west jet stream in the middle troposphere (~500 hPa) and the presence of the unstable layer between 600 and 400 hPa isobar [10]. The first pattern appeared at Menorca Island, Spain, in the west of the Mediterranean Sea, and the area of the wave propagation moved eastward [10]. The area of the high wind speed in the middle troposphere was located east of the trough.

The cold or dry sector of the cold or stationary front can satisfy the wave-CISK or wave-duct structure very well. In February 2009 event in the west Kyushu in **Figure 13**, Japan, a train of the pressure wave was generated in the north sector of the stationary front under both mechanisms of wave duct and wave CISK. The warm moist air lifted by the mountain effect in South China mixed with the dry air of the mid-troposphere from the south of the Himalaya mountain range. The mixed air generated the unstable layer in the mid-troposphere and covered above the East China Sea. The trough extended from the Siberia and the subtropical high-pressure system generated the latitudinal convergence over the area of the unstable mid-troposphere [26]. The wave length of the pressure waves ranged 30–100 km with the period of 20–60 min including the eigen oscillation mode in various bays in that area.

http://dx.doi.org/10.5772/63762

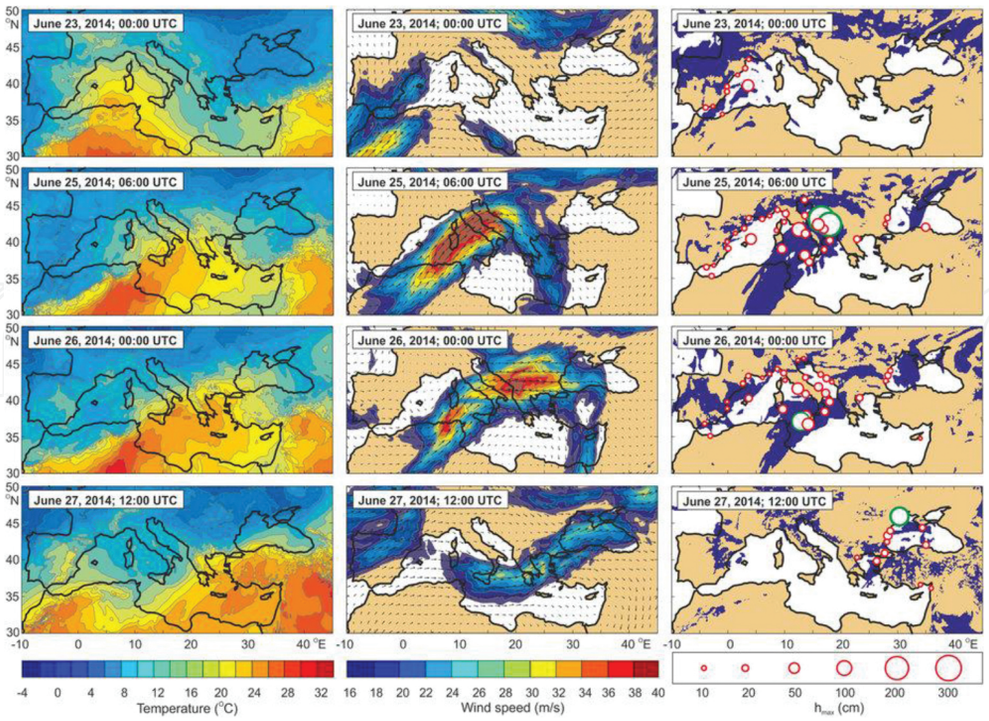


**Figure 12.** Propagation of the meteotsunamigenic synoptic pattern of 2014 together with the maximum heights of corresponding sea level oscillations at the times of the meteotsunami events. Left panels are 850 hPa air temperature, middle panels are 500 hPa wind and right panels are distribution of the unstable layer (Ri <0.25) in the mid-troposphere. (Šepić et al., 2015) [10].

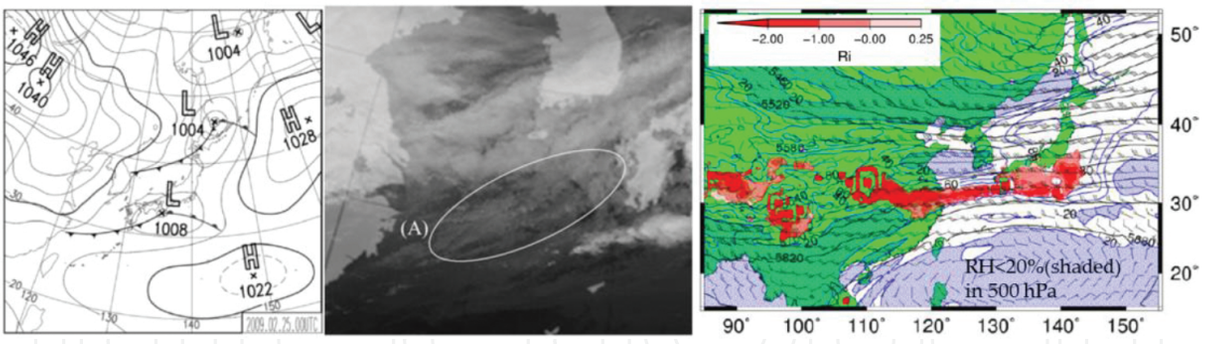


**Figure 13.** Weather condition of meteorological tsunami around the cold front on February 25, 2009. The surface weather chart (left), wavy clouds by satellite IR image (middle) and unstable layer covered with the East China Sea (right) [26].

## 7. Discussion and conclusion: the predictability of meteorological tsunami

The recent studies on meteorological tsunami presented that much more larger-scale motions played an important role in forming the atmospheric structures to generate meso-β or γ-scale

disturbances at sea level. Some latest papers pointed the importance of the (sub-) seasonal scale variation propagating from lower to mid-latitude.

Those findings in larger-scale motion will provide the capability for the prediction of the meteorological tsunamis from atmospheric and oceanographic aspects. It should be noticed that there have been much advances in technologies on observation, numerical modelling and others to make progresses scientifically in meteorological tsunamis. Especially, the high-performance computing technology brings us huge benefits to resolve the pressure disturbance in using numerical model such as the weather forecasting and research (WRF) model [46]. **Figure 14** illustrates a framework on the prediction of the meteorological tsunami. In obtaining a first guess, it is better to start the weather forecast in the synoptic scale with the duration of 2 or 3 days to make a first guess on the stability structure related to the wave duct or wave CISK. And then the downscaling run executes to resolve the atmospheric (mainly pressure) disturbance at sea level.

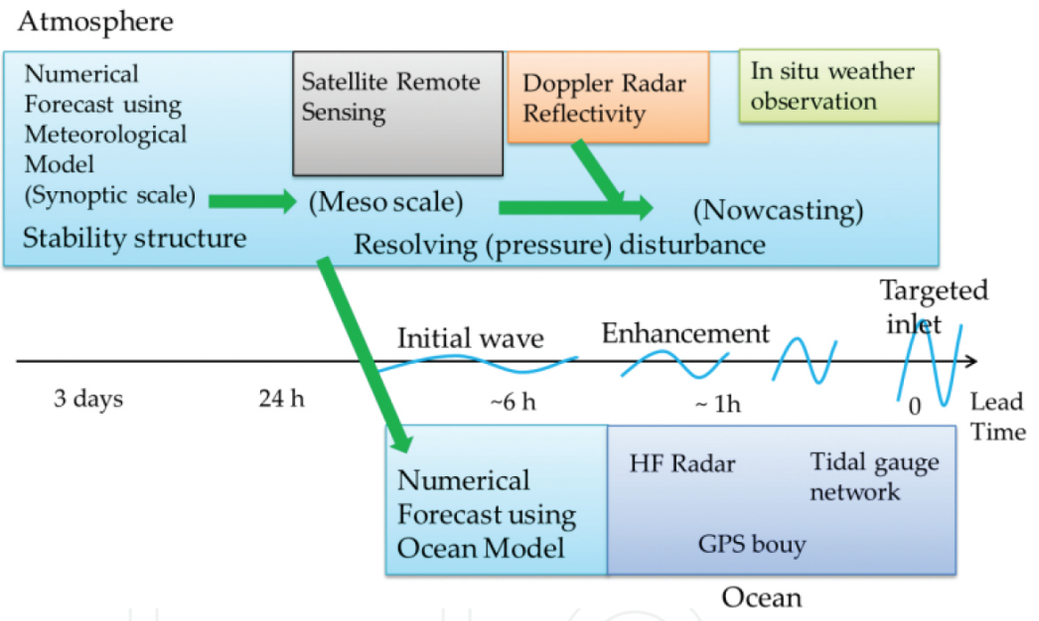


**Figure 14.** A framework on the prediction of the meteorological tsunami.

The infrared images of the satellite remote sensing have useful information if the sequence of the wavy clouds in the mid-troposphere moves fast over the ocean satisfying the Proudman resonance. A new geostationary meteorological satellite named Himawari-8 stated the operation in Asia-Australian region since July 2015. The Himawari-8 has 16-image channels of visible, near infrared, infrared bands, with the horizontal resolution of 0.5 (visible) to 2 km (infrared). The scan interval is every 10 min for global mode, and every 2.5 min for Japan area. The target such as typhoon or hurricane also scans for every 2.5 min for necessity. It will be much easier to see the propagation of the atmospheric wave using satellite data.

Although the mesoscale model can resolve the pressure disturbance to a considerable extent, it is not easy to apply directly into the ocean models as a surface boundary condition, because

of the difficulty in giving enough accuracy as compared to the in situ observation. Even small errors of the location, wave length, frequency, the propagation direction, etc. might affect the amplitude in the inlet. Indeed, Renault et al. (2011) [47] is the first to succeed the meteotsunami simulation by coupling of the WRF and ROMS (regional ocean modelling system) [48]. But the results of the pressure disturbance from the meteorological model should be treated very carefully. If the powerful computing resource is available, it is desirable to execute the ensemble run using various initial conditions, cloud physics parameter and boundary layer options for checking the uncertainty of the model behaviour.

The enhancement of the in situ observation network is one of the ways to provide a short-term prediction or real-time warning, in which the lead time is shorter than 1 h in many situations. It is convenient to install the automated station on isolated islands around the targeted area such as Adriatic Sea [49]. However, it seems not to be applicable such as US East Coast. The high-frequency (HF) radar extends the possibility for monitoring the meteorological tsunami propagation. Lipa et al. (2014) [50] detected the wave up to 23 km offshore, 47 min before reaching the shoreline by the analysis of HF radar signals on the June 2003 event on the US East Coast.

Indeed, further developments are required to get more accurate outputs for linking each processes, but we can believe that the day will come to predict the meteorological tsunami in a practical manner.

## Author details

Kenji Tanaka* and Daiki Ito

*Address all correspondence to: k.tanaka.pb@cc.it-hiroshima.ac.jp

Department of Global Environment Studies, Faculty of Environmental Studies, Hiroshima Institute of Technology, Hiroshima, Japan

## References

[1] Monserrat S., I. Vilibić, A.B. Rabinovich. Meteotsunamis: atmospherically induced destructive ocean waved in the tsunami frequency band. Nat. Hazards Earth Syst. Sci. 2006;6:1035–1051.

[2] Defant A. Physical Oceanography. New York, Oxford, London and Paris: Pergamon Press; 1962. pp. 234–235.

[3] Nomitsu T. A theory of tsunamis and seiches produced by wind and barometric gradient. Mem. Coll. Sci. Imp. Univ. Kyoto A. 1935;18:201–214.

[4] Proudman J. The effects on the sea of changes in atmospheric pressure. Geophys. J. Intl. 1929;2:197–209.

[5] Hibiya T., K. Kajiura. Origin of 'Abiki' phenomenon (kind of seiches) in Nagasaki Bay. J. Oceanogr. Soc. Jpn. 1982;38:172–182.

[6] Synolakis C.E. Green's law and the evolution of solitary waves. Phys. Fluids A. 1991;3(3):490–491.

[7] Greenspan H.P. The generation of edge waves by moving pressure distributions. J. Fluid Mech. 1956;1;574–592.

[8] Honda K., T. Terada, Y. Yoshida, D. Ishitomi. An investigation on the secondary undulation of oceanic tides. J. College Sci. Univ. Tokyo. 1908;24:113p.

[9] Rabinovich A.B. Seiches and harbor oscillations. In: Kim, Y.C., editors. Handbook of Coastal and Ocean Engineering. Singapore: World Scientific Publ.; 2009. pp. 193–236.

[10] Šepic J., I. Vilibić, A.B. Rabinovich, S. Monserrat. Widespread tsunami-like waves of 23–27 June in the Mideierranean and Black Sea generated by high-altitude atmospheric forcing. Sci. Rep. 2015;5:11682(8p.). DOI:10.1038/srep11682

[11] Vilibić I., J. Šepić. Desctructive meteotsunamis along the eastern Adriatic coast: overview. Phys. Chem. Earth. 2009;34:904–917.

[12] Vilibić I., S. Monseratt, A.B. Rabinovich, H. Mihanović. Numerical Modelling of the destructive meteotsunami of 15 June 2006 on the coast of the Baleatic Islands. Pure Appl. Geophys. 2008;165:2169–2195.

[13] Pattiaratchi I., C.B., E.M.S. Wijeratne. Are meteotsunamis an underrated hazard? Phil. Trans. R. Soc. A. 2015;373:20140377 (23p.). DOI: 10.1098/rsta.2014.0377

[14] Haslett S.R., H.E. Mellor, E.A. Bryant. Meteo-tsunami hazard associated with summer thunderstorms in the United Kingdom. Phys. Chem. Earth. 2009;34:1016–1022.

[15] de Jong M.P.C., L.H. Holtsuijsen, J.A. Battjes. Generation of seiches by cold fronts over the southern North Sea. J. Geophys. Res. 2003;104(C4):3117(10p.). DOI: 10.1029/2002JC001422

[16] Renqvist H. Ein Seebär in Finnland, Zur Frage Nach der Entstehung der Seebären. Geogr. Ann. 1926;8;230–236.

[17] Meteogroup in Netherlands. 'Meteotsunami' aan Nederlandse kust http://www.weer.nl/nieuws/detail/2012-01-04-meteotsunami-aan-nederlandse-kust/ (last view on Mar. 26, 2016).

[18] Wadgidsen web: Meteo-tsunami aan Nederlandse Kust 3 Januari 2012. http://wadgidsenweb.nl/nieuwsarchief/waddenzee2007-2012/536-meteo-tsunami.html, Updated on Feb. 5, 2012 (last view on Mar. 26, 2016).

[19] Ewing M., P. Rauhala, K.K. Kahma, T. Stipa, H. Boman, A. Kangas. Recent observations on the Finnish Coast. Nat. Hazards. 2014;74:197–215.

[20] Paxton C.H., D.A. Sobien. Resonant interaction between an atmospheric gravity wave and shallow water wave along Florida's West Coast. Bull. Amer. Meteor. Soc. 1998:79(12):2727–2732.

[21] Churcill D.D., S.H. Houston, N.A. Bond. The Daytona beach wave of 3–4 July 1992: a shallow-water gravity wave forced by a propagating squall line, Bull. Am. Meteor. Soc. 1995;76(1):21–32.

[22] Šepić J., A.B. Rabinovich. Meteotsunami in the great lakes and on the Atlantic coast of the United States generated by the 'derecho' of June 29–30, 2012. Nat. Hazards. 2014;74:75–107.

[23] Ewing M., F. Press, W.L. Donn. An exaplanation of the lake Michigan wave of 26 June 1954. Science. 1954;120:684–686.

[24] Thomson R.E., A.B. Rabinovich, I.V.Fine, D.C. Sinott, A. McCarthy, N.A.S. Sutherland, L.K. Neil. Meteorological tsunamis on the coasts of British Columbia and Washington. Phys. Chem. Earth. 2009;34:971–988.

[25] Akamatsu H. On seiches in Nagasaki Bay. Pap. Meteor. Geophys. (Meteorological Research Institute, Japan Meteorological Agency). 1982;33(2):95–115.

[26] Tanaka K. Atmospheric pressure-wave bands resulted in meteotsunami over the East China Sea on February 2009. Nat. Hazards Earth Syst. Sci. 2010;10(12):2599–2610.

[27] Ito D. On meteorological systems related to meteorological tsunamis over the East China Sea. Master Thesis, Hiroshima Institute of Technology. Hiroshima, Japan, 2016:138.

[28] Asano T., T. Yamashiro, N. Nishimura. Field observations of meteotsunami locally called 'abiki' in Urauchi Bay, Kami-Koshiki Island, Japan. Nat. Hazards. 2012;64:1685–1706.

[29] Tanaka K., S. Gohara, T. Koga, R. Yamaguchi, F. Yamada. Abiki oscillations in Sakitsu Bay, west Kyushu, Japan. Nat. Hazards. 2014;74:233–250.

[30] Tanaka K. On meteotsunamis around Tsushima Straits generated by the Baiu front. Nat. Hazards. 2012;63:805–822.

[31] Cho K-H., J-Y. Choi, K-S. Park, S-K. Hyun, Y. Oh, J-Y. Park. A synoptic study on tsunami-like sea level oscillations along the west coast of Korea using an unstructured-grid ocean model. J. Coastal Res. 2013;65:678–683.

[32] Wang X., K. Li, Z. Yu, J. Wu, Statistical characteristics of seiches of Longkou harbour. J. Phys. Oceanogr. 1987;17:1963–1966.

[33] Makarenko E., T. Ivelskaya. Meteotsunmai in the ports of Sakhalin region from the observational telemetry network of TWS. Navigation and Marine Researches, selected

reports of the 3rd Sakhalin regional marine scientific conf. Feb. 15–16, 2011: 205–210. ISSN 2227-4375.

[34] Pattriaratchi C., E.M.S. Wijeratne. Observations of meteorological tsunamis along the south-west Australian coast. Nat. Hazards. 2014;74:280–302.

[35] Goring D.G. Extracting long waves from tide-gauge records. J. Waterway Port Coast Ocean Eng. ASCE. 2008;134:306–312.

[36] Okal E.A., Y.NJ. Visser, C.H. de Beer. The Dwaskersbos, South Africa local tsunami of August 1969: field survey and simulation as a meteorological event. Nat. Hazards. 2014;74:251–268.

[37] Wertman C.A., R.A. Yabnosky, S. Yang, J. Merril, C.R. Kincaid, R.A. PackalMesoscale convective system surface pressure anomalies responsible for meteotsunamis along U.S. East Coast on June 13th, 2014. Sci. Rep.;9:7143(9p.). DOI: 10.1038/srep071

[38] NOAA Pacific Tsunami Warning Centre. Meteotsunami Animation: U.S. East Coast June 2013. https://www.youtube.com/watch?v=ykABRe5Yt3c.Uploaded on Dec. 8, 2013 (last view on Mar. 28, 2016).

[39] Kobayashi S., Y. Ota, Y. Harada, A. Ebita, M. Moriya, H. Onoda, K. Onogi, H. Kamahori, C. Kobayashi, H. Endo, K. Miyaoka, K. Takahashi. The JRA-55 reanalysis: general specifications and basic characteristics. J. Meteor. Soc. Jpn. 2015;93:5–48.

[40] Lindzen R.S., K.K. Tung. Banded convective activity and ducted gravity waves. Mon. Weather Rev. 1976;104:1602–1617.

[41] Lindzen R.S. Wave-CISK in the tropics. J. Atmos. Sci. 1974;31:156–179.

[42] Monserrat S., A.J. Thorpe. Using a ducting theory in an observed case of gravity waves. J. Atmos. Sci. 1996;53:1724–1736.

[43] Vilibić I., K. Horvath, N.S. Mahović, S. Monserrat, M. Maros, A. Amores, I. Fine. Atmospheric process responsible for generation of the 2008 Boothbay meteotsunami. Nat. Hazards. 2014;74:29–52.

[44] Lin Y.-L. Mesoscale dynamics. Cambridge: Cambridge University Press; 2007. p. 630.

[45] Belušić D., B. Grisono, Z.B. Kraić. Atmospheric origin of devastating coupled air-sea event in the east Adriatic. J. Geophys. Res. 2007;112:D17111. DOI:10.1029/2006JD008204

[46] Skmarock W.C., J.B. Klemp, A time-split nonhydrostatic atmospheric model for weather research and forecasting applications. J. Comput. Phys. 2008;227:3465–3485.

[47] Renault L., G. Vizono, A. Jansa, W.J. Tintore, Toward the predictability of meteotsunamis in the Balearic Sea using regional nested atmosphere and ocean models. Geophys. Res. Lett. 2011;38:L10461. DOI:10.1029/2011GL047361

[48] Shcheptickin A.F., J.C. McWilliams. The regional oceanic modelling system (ROMS): a split-explicit, free-surface, topography-following-coordinate ocean model. Ocean Modell. 2005;9:347–404.

[49] Šepić J., I. Vilibić. The development and implementation of a real-time meteotsunami warning network for the Adriatic Sea. Nat. Hazard Earth Syst. Sci. 2011;11:83–91.

[50] Lipa B., H. Parikh, D. Barrick, H. Roarty, S. Glenn. High frequency radar observation of the June 2013 US East Coast meteotsunami. Nat. Hazards. 2014;74:109–122. DOI: 10.1007/s11069-013-0992-4

IntechOpen

IntechOpen

IntechOpen